frontiers | Frontiers in Environmental Science

ORIGINAL RESEARCH
published: 22 July 2022
doi: 10.3389/fenvs.2022.953509

Coprecipitation of Organic Matter, Phosphate With Iron: Implications for Internal Loadings of Phosphorus in Algae-Dominated and Macrophyte-Dominated Lakes

JiaRu Dai[1,2], QiaoYing Zhang[2], JingJing Liu[2,3], ShuaiLong Wen[2,3], YuFeng Zhang[1], Ding He[4] and YingXun Du[2]**

[1]School of Environmental Science and Engineering, Nanjing Tech University, Nanjing, China, [2]State Key Laboratory of Lake Science and Environment, Nanjing Institute of Geography and Limnology, Chinese Academy of Sciences, Nanjing, China, [3]University of Chinese Academy of Science, Beijing, China, [4]Department of Ocean Science and Hong Kong Branch of the Southern Marine Science and Engineering Guangdong Laboratory (Guangzhou), The Hong Kong University of Science and Technology, Hong Kong, Hong Kong SAR, China

OPEN ACCESS

Edited by:
Wei He,
China University of Geosciences, China

Reviewed by:
Peng Zhang,
China University of Geosciences Wuhan, China
Weiying Feng,
Beihang University, China

***Correspondence:**
YingXun Du
yxdu@niglas.ac.cn
YuFeng Zhang
zhangyuf99@126.com

Specialty section:
This article was submitted to Biogeochemical Dynamics, a section of the journal Frontiers in Environmental Science

Received: *26 May 2022*
Accepted: *20 June 2022*
Published: *22 July 2022*

Citation:
Dai J, Zhang Q, Liu J, Wen S, Zhang Y, He D and Du Y (2022) Coprecipitation of Organic Matter, Phosphate With Iron: Implications for Internal Loadings of Phosphorus in Algae-Dominated and Macrophyte-Dominated Lakes. Front. Environ. Sci. 10:953509. doi: 10.3389/fenvs.2022.953509

Coprecipitation with iron (Fe) plays an essential role in the biogeochemical cycles of organic carbon (OC) and phosphorus (P) in lakes. The sources and composition of organic matter (OM) mediate its association with iron, which could thus influence the immobilization of phosphorus. In this study, water-soluble organic matter from the sediments of two typical states of shallow lakes, macrophyte-dominated zones (M-WSOM) and algae-dominated zones (A-WSOM), was extracted, and the ternary coprecipitation of WSOM, phosphate with Fe(III), was investigated. The ternary coprecipitation process was enhanced with increasing Fe(III) or decreasing pH value. It was found that pH of 6.5 was more favorable for coprecipitation than a pH of 7.5 or 8.5. At pH 6.5, the complexation between WSOM and Fe(III) occurred at the low Fe(III) inputs, while the coprecipitation of phosphate, WSOM with Fe(III) took place when Fe(III) inputs reached 40 μM. The presence of A-WSOM showed stronger inhibition on the coprecipitation of phosphate than that by M-WSOM. The formed ternary coprecipitates with A-WSOM had lower C/Fe ratios (0.13–2.78) than those with M-WSOM (1.28–4.05), which was because A-WSOM had lower aromaticity than M-WSOM. In addition, more functional groups in A-WSOM could complex with Fe(III), resulting in less immobilization of OC and P during the coprecipitation of A-WSOM, phosphate, and Fe(III). Our results demonstrated that in algae-dominated zones, more phosphorus remained soluble during the ternary coprecipitation, which could perform positive feedback on the growth of phytoplankton and provide a novel explanation for the difficulty in restoring eutrophic lakes.

Keywords: sedimentary water-soluble organic matter, sediment-water interface, carbon sink, shallow lakes, pH value, C/Fe ratio

1 INTRODUCTION

Lake sediments receive a large amount of organic carbon (OC) from overlying water, mainly including terrestrial organism residues and soil organic matter imported from the basin area, as well as the residues of macrophytes, algae, and bacteria in the lake (Lai et al., 2020). Lake sediments are important carbon sinks since the annual buried organic carbon (OC) in global lakes accounts for ~50% of that in the ocean, while the area of lakes is only 4% of the terrestrial surface area (Dean and Gorham, 1998; Verpoorter et al., 2014). Furthermore, the association of organic matter (OM) with minerals resulted in long-term burial of OC in lake sediments (Kleber et al., 2015) since the association of organic matter (OM) with minerals can protect OC from utilization by bacteria and mineralization (von Lutzow et al., 2006).

Iron (Fe)-bound OM is a vital proportion (21.5 ± 8.6%) of OC in sediments in diverse aquatic circumstances such as oceans, estuaries, and lakes (Lalonde et al., 2012). The association of OM with Fe (hydr)oxides *via* adsorbing onto iron-containing minerals or coprecipitating with ferric ion [Fe(III)] plays a key role in the immobilization of dissolved organic matter (DOM) in aquatic ecosystems (Sowers et al., 2019). Coprecipitation of DOM with Fe(III) is defined as the settling down of DOM accompanying with ferric ion's precipitation *via* inclusion, occlusion, or adsorption (Mikutta and Kretzschmar 2008; Eusterhues et al., 2011). Compared to adsorption, coprecipitation is a more important pathway for forming iron-bound OM since coprecipitation can immobilize much more OC than adsorption (Luo et al., 2021; Luo et al., 2022). Moreover, the formed coprecipitates are more stable than the adsorption complexes because of their compact structure (Chen et al., 2014). Sources and composition of OM mediate its ability to coprecipitate with iron-bearing minerals (Eusterhues et al., 2011; Chen et al., 2014; Han et al., 2019). For instance, high aromatic and high-molecular-weight organic compounds were preferentially coprecipitated with Fe(III) (Du et al., 2018). The association of OM with iron is competed by co-existing anions such as phosphate. Previous studies demonstrated that phosphate and the terrestrially derived OM could both coprecipitate with Fe(III), and both performed an inhibitory effect on each other during the coprecipitation with ferric ions (Luo et al., 2022). As it is well known, P is one of the essential nutrients for aquatic biota and the limiting nutrient for phytoplankton growth (Conley et al., 2009). The internal loading of phosphorus has been considered a primary factor in maintaining lake eutrophication (Sondergaard et al., 2001). Iron-bound phosphorus accounts for ~30% of total phosphorus in sediments and is regarded as the mobile phosphorus since it is readily reduced and released into the overlying water (Sondergaard et al., 2001). As discussed earlier, OM composition, which controls the coprecipitation of OM with iron, could also influence the immobilization of phosphorus during the ternary coprecipitation of OM-Fe-P.

There are two typical states of shallow lakes: macrophyte-dominated lakes (clear state) and algae-dominated lakes (turbid state), which have distinct DOM sources (macrophyte or phytoplankton) and compositions. Macrophyte is regarded as the key factor in maintaining the clear state of shallow lakes. With the development of eutrophication, the growth of phytoplanktons is accelerated, which results in the turbid state and thus the disappearance of macrophytes due to light limitation (Scheffer et al., 1993; Scheffer et al., 2001). It was found that algae-derived DOM contains more lipid compounds, while macrophyte-derived DOM was dominated by lignin and tannin compounds (Liu et al., 2020). The diverse composition of DOM from macrophytes and algae affects the OM in the macrophyte-dominated and algae-dominated zones, both the lake water and the sediments. In our previous study (Du et al., 2022), the water-soluble organic matter (WSOM) in the sediments from the macrophyte-dominated and algae-dominated zones in Taihu Lake was characterized. It was found that WSOM in the sediments of macrophyte-dominated lake area had a higher relative molecular weight and higher aromaticity. In contrast, WSOM in the sediments of algae-dominated lake area had a higher content of protein-like components and more proteins.

Due to the different origins and properties of OM in the algae-dominated and macrophyte-dominated lakes, it was hypothesized that in the coprecipitation of OM with Fe, the interaction between OM and P during the coprecipitation with Fe would also be different in these two typical states of lakes. Such information is critical for understanding the OC sequestration and potential P release in the two typical states of shallow lakes. Therefore, in this study, WSOM was extracted from the sediments of macrophyte-dominated and algae-dominated zones in Taihu Lake, and the coprecipitation reaction of DOM, Fe, and P was investigated to reveal the difference in carbon and phosphorus immobilization by Fe coprecipitation in the two typical states of shallow lakes.

2 MATERIAL AND METHODS

2.1 Extraction of Water-Soluble Organic Matter From the Sediments in Algae-Dominated and Macrophyte-Dominated Zones

The surface sediments (from the top 10 cm) were collected in the summer of 2019, from the macrophyte-dominated zone of East Taihu Lake (31°2′3″ N, 120°25′47″ E) and the algae-dominated zone of Meiliang Bay (31°26′3″ N, 120°11′18″ E). The sediments were freeze-dried, ground, and homogenized. The content of TOC, TN, TP, and metal elements for the two types of sediment was listed in **Supplementary Table S1**. Sediments in the algae-dominated zone had a lower molar ratio of C:N (7.5) than that in the macrophyte-dominated zone (8.8).

Water-soluble organic matter was extracted from sediments of the macrophyte-dominated zone (M-WSOM) and algae-dominated zone (A-WSOM)

Briefly, a certain amount of sediment was added to ultrapure water at a ratio of 1:10 (100 g: 1,000 ml). Then, after oscillating at an isothermal shaker at 25°C and for 24 h, the sediment–water mixture was centrifuged at 4,000 rpm. The supernatant collected

TABLE 1 | Conditions of coprecipitation of DOM, Fe, and P.

Group	DOC (mg/L)	Fe (μM)	P (μM)	pH
M-WSOM	6	0, 5, 10, 20, 40, 60, and 100	30	6.5, 7.5, and 8.5
A-WSOM	6	0, 5, 10, 20, 40, 60, and 100	30	6.5, 7.5, and 8.5
No WSOM	—	0, 5, 10, 20, 40, 60, and 100	30	6.5, 7.5, and 8.5

was then filtered using a 0.2-μm membrane filter (Millipore, GVWP02500). Because WSOM extracted from former steps may have many ions such as metals and phosphate, which may disturb the coprecipitation experiments, the solid-phase extraction method (SPE) *via* PPL column was used to purify WSOM (Dittmar et al., 2008; Wang et al., 2020; Zhou et al., 2020).

2.2 Coprecipitation Experiments

The coprecipitation reaction of WSOM, Fe, and P was carried out to investigate the influence of WSOM source, reaction pH, and Fe dosage. Coprecipitation experiments were carried out at various pH values (pH of 6.5–8.5) and Fe(III) dosage (0–100 μM) as listed in **Table 1**. The ternary coprecipitation experiments of WSOM-Fe-P were conducted in a batch of 100-ml brown glass bottles by adding 50 ml of phosphate (30 μM) and WSOM (6 mg C/L) mixture with the desired pH value (6.5, 7.5, and 8.5), followed by adding different volumes of Fe(III) (prepared as $FeCl_3$ stock solution, pH = 2.6, with additional volumes ≤100 μL). No pH buffer was used in the experiments, considering that the common pH buffer of phosphate-containing solution or the organic pH buffer of HEPES would interfere with the coprecipitation reaction. The mixture was oscillated in an isothermal shaker at 25°C and 200 rpm for 24 h and then filtered through a 0.22-μm membrane (Millex-GP). It was found that the change of pH in the supernatant after 24 h was minor. The filtrates were stored at 4°C and measured within 3 weeks. To evaluate the effect of WSOM on P precipitation, a blank experiment of binary coprecipitation of Fe-P was also investigated, the procedure of which was the same as that of WSOM-Fe-P described earlier, without the addition of WSOM. Our previous experiments on the coprecipitation of terrestrially derived HA, Fe, and P (Luo et al., 2022) showed that the standard error (triplicates) for residual DOC, Fe, and P percentages was always within 5%. Also, due to the small quantity of purified WSOM, each experiment was conducted once.

2.3 Analytical Methods

DOC concentration (mg C/L) of WSOM was measured using the high-temperature combustion method on a total organic carbon analyzer (TOC-V CPN, Shimadzu, Japan). Concentrations of phosphate and Fe were measured by the malachite green chromogenic method (Hashitani and Okumura 1987) and the ferrozine colorimetric method (Stookey 1970) using a spectrophotometer (Lambda 35, Perkin-Elmer, United States), respectively.

The absorption spectra of the filtrates were scanned between 200 and 800 nm at 1-nm intervals using a UV–Vis spectrophotometer (Lambda 35, Perkin-Elmer, United States) with Milli-Q water as the blank. The absorption spectra were used for the correction of the raw EEM data and also to characterize the initial WSOM (**Supplementary Figure S1**). $SUVA_{254}$, which is calculated as the ratio of the absorbance at 254 nm to DOC concentration, and is common as a surrogate of DOM aromaticity. It was found that M-WSOM has a higher $SUVA_{254}$ value (1.55 L/(mg C m) vs. 1.39 L/(mg C m)) than A-WSOM.

Fluorescence EEMs were collected using a fluorescence spectrometer (F-7000, Hitachi High Technologies, Japan). Excitation (Ex) wavelengths ranged from 200 to 450 nm at 5-nm intervals, and emission (Em) wavelengths were from 250 to 550 nm at 1-nm intervals. Several post-acquisition steps were carried out for the correction and standardization of EEMs: 1) inner filter effect that was corrected by using the absorption spectra (McKnight et al., 2001); 2) blank correction by subtracting the EEM spectra of Milli-Q water; and 3) calibration and normalization of daily fluorescence intensity variations using Milli-Q water Raman units. A PARAFAC model including all M-WSOM and A-WSOM samples ($n = 75$) was established using the DOM Fluor toolbox in MATLAB R2008a (Stedmon and Bro 2008). A four-component model generated the fluorescence intensity (Fmax, unit = R.U.) of four components for each sample. The model was validated using split-half analysis and random initialization. Component 1 (C1) and component 3 (C3) were identified as microbially derived humic-like and terrestrial humic-like substances, respectively (**Supplementary Table S2**). Component 2 (C2) and component 4 (C4) were assigned as protein-like compounds of tryptophan-like and tyrosine-like substances, respectively. For the original M-WSOM, the relative abundance of C1–C4 to the total fluorescence intensity was 34.17, 28.19, 19.89, and 17.76%, respectively. Also, those for A-WSOM was 29.48, 33.27, 17.49, and 19.76%, respectively. M-WSOM contained more humic-like substances but less protein-like substances than A-WSOM. Humification index (HIX) was calculated based on the corrected EEMs, which is the ratio of the mean value of the fluorescence intensity between the emission at 435–480 nm and that at 300–345 nm, both excited at the excitation wavelength of 254 nm. HIX can characterize the humification degree of organic matter (Zsolnay et al., 1999).

The residual percentage of Fe(III) (or phosphate, DOC) was calculated as the percentage of the concentration of Fe(III) (or phosphate, DOC) in solution after coprecipitation to its initial input. It is noted that the residual percentage of Fe(III) was not provided since it cannot be calculated when Fe (III)'s dosage was 0 μM. The inhibitory effect of WSOM on P coprecipitation was measured as the difference in phosphate's residual percentage between binary coprecipitation of Fe-P (in the absence of WSOM) and ternary coprecipitation of Fe-WSOM-P.

The OC, Fe, and P contents in coprecipitates were determined *via* the difference in concentrations of dissolved phase species

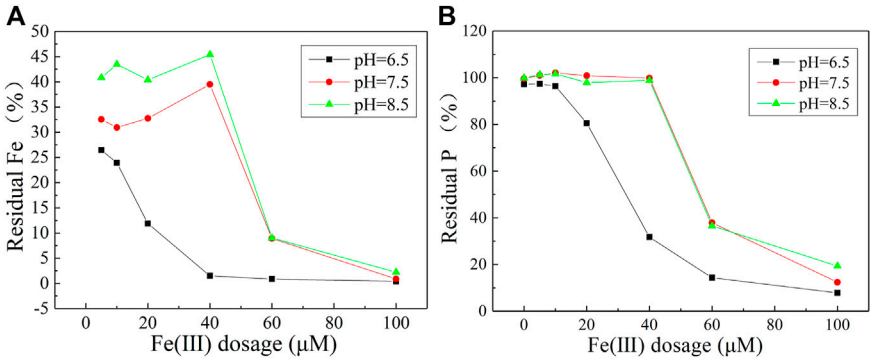

FIGURE 1 | Residual percentage of Fe(III) **(A)** and PO_4^{3-} **(B)** at the end of precipitation reaction in the absence of WSOM.

before and after reactions of the concentrations in solutions due to the following consideration. Due to the short term (24 h) for the experimental period and the sterile environment (the solution was filtered through 0.22 μm), the microbial metabolism of WSOM could be ignored during the reaction. Thus, the total mass of the dissolved and particulate Fe, P, and WSOM after the reaction was the same as that before the reaction.

3 RESULTS

3.1 Binary Coprecipitation of P With Fe

The precipitation of P with Fe increased with pH decrease or Fe(III) dosage increase in the binary coprecipitation of phosphate with Fe(III) (**Figure 1**). When pH was 6.5, the residual percentage of PO_4^{3-} was lower than that of pH = 7.5 and 8.5. With the Fe(III) dosage increased, the remaining Fe(III) and PO_4^{3-} concentrations in the solution gradually decreased. When pH was 6.5 and the Fe(III) dosage was less than 10 μM, the concentration of PO_4^{3-} remained unchanged, and the concentration of Fe(III) decreased by ~75%. When the Fe(III) dosage increased to over 40 μM, PO_4^{3-} and Fe(III) concentrations decreased sharply. When the Fe(III) dosage reached 100 μM, the residual PO_4^{3-} was 7.8% (pH = 6.5), 12.4% (pH = 7.5), and 19.3% (pH = 8.5), and almost all Fe(III) was precipitated.

At pHs 7.5 and 8.5, the change tendency of residual Fe(III) and PO_4^{3-} with the Fe(III) dosage was similar. When the Fe(III) dosage was less than 40 μM, the PO_4^{3-} concentration was almost unchangeable, while the Fe(III) concentration decreased by 65% (pH = 7.5) and 55% (pH = 8.5). At this time, the precipitation of Fe was mainly caused by the formation of iron hydroxides. When the Fe(III) dosage was more than 40 μM, the residual PO_4^{3-} decreased gradually, indicating that PO_4^{3-} coprecipitated with Fe(III).

3.2 Ternary Coprecipitation of WSOM, P With Fe

3.2.1 Effects of Reaction pH on Ternary Coprecipitation of WSOM-Fe-P

For M-WSOM, with the increase of pH values (from 6.5 to 8.5), the residual percentage of Fe(III), PO_4^{3-}, and DOC in the solution gradually increased (**Figures 2A–C**).

At pH = 6.5, when the dosage of Fe(III) was less than 20 μM, about ~30% Fe(III), and almost all PO_4^{3-}, DOC remained in the solution. Beyond 20 μM, the remaining Fe(III) and P decreased linearly, and at Fe(III) of 100 μM, the residual percentage of Fe(III) and P was 2% and 13%, respectively. While for DOC, the residual percentage decreased rapidly to 76% at Fe(III) of 40 μM and then gradually to 67% when Fe(III) dosage reached 100 μM.

When pH increased to 7.5, it was found that the precipitation of Fe(III) became weaker, as well as the coprecipitation of WSOM and phosphate. The remaining Fe(III) ranged from 40 to 50% when the Fe(III) dosage was less than 60 μM, but it decreased to 6% at Fe(III) dosage of 100 μM. Concerning P and DOC, no obvious coprecipitation of P was observed when Fe(III) was no more than 40 μM, while coprecipitation of DOC (~10%) was observed at Fe(III) of 40 μM. The residual P and DOC decreased gradually to 30 and 76%, respectively, when Fe(III) dosage was increased to 100 μM.

When the pH was 8.5, no decrease of PO_4^{3-} and DOC concentrations in the solution was observed, which meant that no coprecipitation of them with Fe(III) happened. Under this condition, the residual percentage of Fe(III) was maintained within the range of 40–60%.

Similar to that with M-WSOM, the coprecipitation of P and A-WSOM with Fe(III) was most distinct at pH 6.5, but the effect of pH showed a relatively weak influence on the change of coprecipitation of Fe(III) and P (**Figures 2D, E**). Only a weak decrease of DOC with the increase of Fe(III) dosage was observed at pH 6.5, while no decrease of DOC at pHs 7.5 and 8.5 (**Figure 2F**) happened.

Table 2 lists the molar ratios of C/Fe and P/Fe for the initial input and the formed coprecipitates. Since no coprecipitation occurred when Fe(III) dosage was less than 20 μM, only ratios of C/Fe and P/Fe at Fe(III) dosages of 40, 60, and 100 μM were listed. With the increase in pH values, the C/Fe and P/Fe ratios gradually decreased. Almost all C/Fe in the coprecipitates were >1. For M-WSOM, the ratios of C/Fe in coprecipitates ranged from 1.28 to 4.05, and the maximum of 4.05 was formed under the conditions of pH = 6.5 and Fe(III) = 40 μM. The ratios of P/Fe in coprecipitates ranged from 0.01 to 0.33, and the maximum of 0.33 was formed under the conditions of pH = 6.5 and Fe(III) =

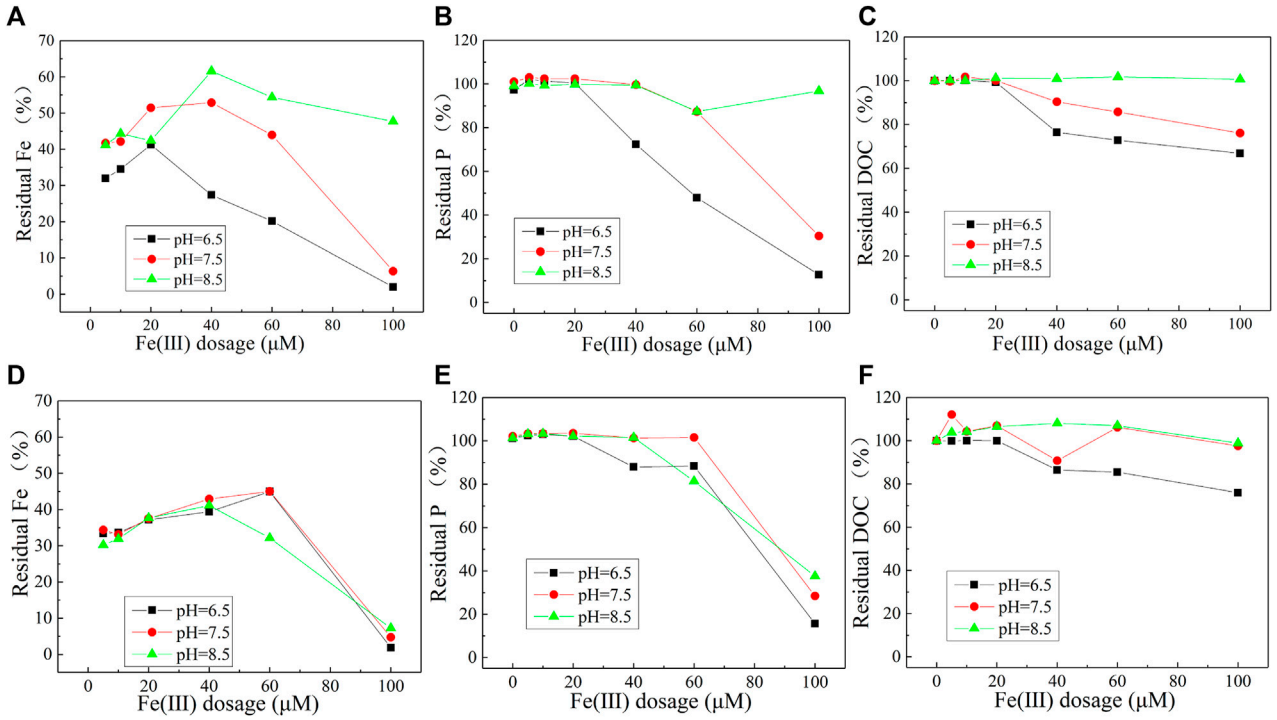

FIGURE 2 | Residual percentage of Fe (III) **(A)**, PO_4^{3-} **(B)**, and DOC **(C)** after coprecipitation of M-WSOM with Fe and P at different pH values and residual percentage of Fe (III) **(D)**, PO_4^{3-} **(E)**, and DOC **(F)** after A-WSOM coprecipitated with Fe and P at different pH values.

TABLE 2 | Comparison in ratios of C/Fe and P/Fe between initial input and coprecipitates under different pHs.

	pH	Initial Fe (μM)	C/Fe (initial input)	P/Fe (initial input)	C/Fe (in coprecipitates)	P/Fe (in coprecipitates)
M-WSOM	6.5	40	12.5	0.75	4.35	0.29
		60	8.33	0.5	3.05	0.33
		100	5	0.3	1.81	0.27
	7.5	40	12.5	0.75	2.50	0.02
		60	8.33	0.5	2.08	0.12
		100	5	0.3	1.25	0.23
	8.5	40	12.5	0.75	—	0.01
		60	8.33	0.5	—	0.13
		100	5	0.3	—	0.02
A-WSOM	6.5	40	12.5	0.75	2.78	0.15
		60	8.33	0.5	2.19	0.11
		100	5	0.3	1.22	0.26
	7.5	40	12.5	0.75	2.06	—
		60	8.33	0.5	—	—
		100	5	0.3	0.13	0.23
	8.5	40	12.5	0.75	—	—
		60	8.33	0.5	—	0.14
		100	5	0.3	—	0.20

60 μM. Increasing Fe(III) dosages resulted in a decrease of the C/Fe ratio in the coprecipitates, while changes in the P/Fe ratio in coprecipitates with increasing Fe(III) dose were not consistent.

For A-WSOM, the molar ratios of C/Fe and P/Fe in coprecipitates ranged from 0.13 to 2.78 and 0.11 to 0.26, respectively. Increasing Fe(III) dosages consistently reduced C/Fe ratios but enhanced P/Fe ratios. The maximum of C/Fe of 2.78 in coprecipitates was achieved at pH 6.5 and Fe(III) dosage of 40 μM, while that of P/Fe (0.26) was formed at pH 6.5 and Fe(III) dosage of 100 μM.

The presence of WSOM inhibited the coprecipitation of P, and the inhibition varied with initial Fe(III) dosage and pH and also with the types of WSOM (**Figure 3**). At pH 6.5, the inhibition by WSOM

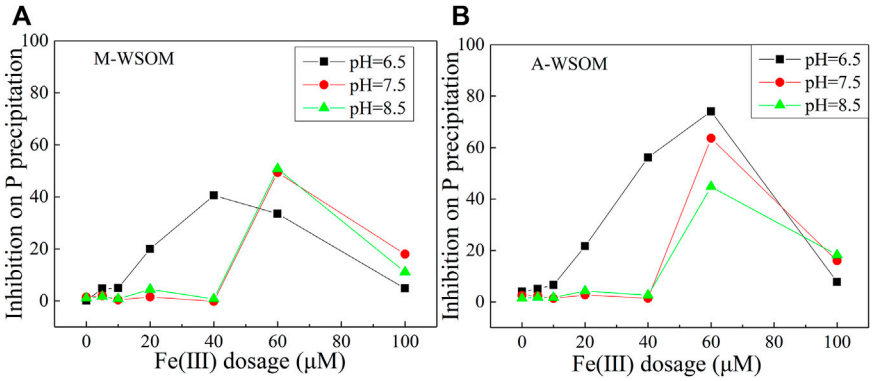

FIGURE 3 | Effects of Fe(III) dosage and pH values on M-WSOM's **(A)** and A-WSOM's **(B)** inhibition of P precipitation.

was observed when Fe(III) ≥ 20 μM. Under the condition of Fe(III) = 20 μM, no coprecipitation of WSOM occurred (**Figure 2C**), and the inhibition by WSOM could be due to enhancement of dissolved Fe and thus the reduction in Fe precipitation. The inhibition of P immobilization by M-WSOM was strongest at Fe(III) dosage of 40 μM and became weaker with further increase of Fe(III) dosage. The coprecipitation of P was inhibited by 0.2–50% in the presence of M-WSOM. At pHs 7.5 and 8.5, the inhibition was strongest at Fe(III) dosage of 60 μM. Combined with **Table 2** (C/Fe ratios), it was observed that Fe(III) dosage served the strongest inhibition on P precipitation (pH 6.5, Fe(III) 40 μM) and corresponded to that with the most effective coprecipitation of M-WSOM (the maximum C/Fe ratio of 4.35). Compared to M-WSOM, the presence of A-WSOM showed stronger inhibition of P immobilization. At pH 6.5, when Fe(III) was 40 and 60 μM, the inhibition of P immobilization by A-WSOM was as high as 60–74%.

3.2.2 Influence of DOM Sources on the Ternary Coprecipitation

The coprecipitation with and without the presence of M-WSOM and A-WSOM was compared at a pH of 6.5 due to the strongest coprecipitation at this pH value (**Figure 4**). In the absence of WSOM, the residual percentage of Fe(III) and P in the solution was both significantly lower than those with WSOM, indicating that the presence of WSOM could inhibit the coprecipitation of Fe-P. The precipitation of Fe(III) by WSOM, could be attributed to the complexation of WSOM with Fe(III) and keeping Fe(III) as the soluble state.

In the presence of WSOM, it was found that all residual percentages of Fe, P, and DOC in the A-WSOM group were higher than those of the M-WSOM group (**Figure 4**). This indicated that the presence of A-WSOM showed stronger inhibition of the coprecipitation process than M-WSOM. While the change tendency of Fe, P, and DOC with Fe(III) dosages in two WSOM groups showed similar patterns. With the Fe(III) dosage increased, the residual percentage of PO_4^{3-} and DOC in the solution showed a decreasing trend. When the Fe(III) dosage was smaller than 20 μM, it is interesting that regardless of the proportion of Fe(III) precipitated (59–68% in the M-WSOM group and 63–67% in the A-WSOM group), no decrease of PO_4^{3-} and DOC in the solution was observed. This implied that at low dosages of Fe(III), no coprecipitation of WSOM or phosphate with Fe(III) happened and the decrease of Fe(III) was due to the formation of $Fe(OH)_3$. When the dosage of Fe(III) was higher than 20 μM, the residual percentage of Fe(III) in the M-WSOM group dropped rapidly, accompanying with the quick decrease of residual P and DOC. For the A-WSOM group, the decrease in residual Fe(III) percentage was observed when Fe(III) dosage was higher than 60 μM, but a slight decrease of DOC and P residual percentage occurred when Fe(III) was higher than 20 μM.

3.3 Fractionation of WSOM During Coprecipitation

Four PARAFAC components in WSOM showed different abilities to coprecipitate with Fe(III). Changes in fluorescence intensity of the four PARAFAC components with increasing iron dosage (pH = 6.5) in M-WSOM and A-WSOM groups (**Figure 5**) showed that the humic-like components (C1 and C3) possessed stronger coprecipitation ability than the protein-like components (C2 and C4), no matter in the M-WSOM or A-WSOM group. Among the four PARAFAC components, the humic-like substance with a long emission wavelength (458 nm) (C3) showed the strongest ability to coprecipitate, and the tyrosine substance of C4 could hardly participate in the coprecipitation. Considering that no coprecipitation of WSOM happened when Fe(III) dosages were less than 20 μM, the decreases in C1 and C3 were possibly due to fluorescence quenching by Fe(III) ion (Yamashita and Jaffé 2008). For M-WSOM, at the Fe(III) dosages of 40–100 μM, the residual percentage of C1, C2, C3, and C4 decreased by 0.4%–14.4%, 2.9%–8.1%, 5.5%–18.3%, and 1.6–8.5%, respectively, compared to that at the Fe(III) dosage of 20 μM. Although the same PARAFAC component, a smaller decrease in fluorescent intensity was observed in the A-WSOM group compared to the M-WSOM group. For A-WSOM, at the Fe(III) dosages of 40–100 μM, the residual percentage of C1, C2, C3, and C4 decreased by 2.8%–12.1%, 1.4%–5.2%, 5.2%–14.9%, and 1.5–13.2%, respectively, compared to that at the Fe(III) dosage of 20 μM.

Changes in HIX (**Figure 5C**) in the supernatant with increasing Fe(III) dosages showed a decreasing tendency for M-WSOM,

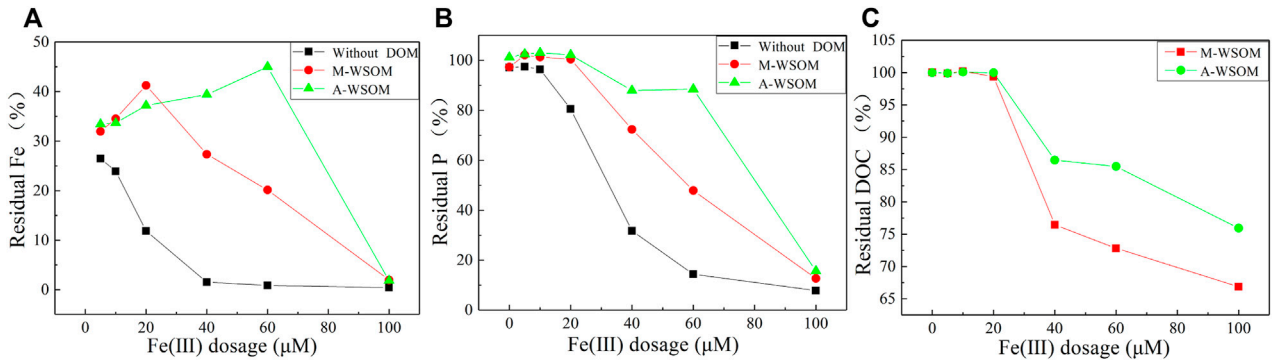

FIGURE 4 | Residual percentage of Fe (III) **(A)**, PO_4^{3-} **(B)**, and DOC **(C)** after coprecipitation of WSOM-Fe-P in sediments from Meiliang Bay, East Taihu Lake (pH = 6.5, DOC = 6 mg/L).

indicating that the coprecipitation led to a decrease in aromaticity. According to the calculation of HIX, which partly corresponded to the ratio of C3 to C2, the quicker decrease in C3 to that in C2 (**Figure 5A**) during the coprecipitation for M-WSOM (Fe ≥ 40 μM) resulted in the decrease of HIX, while the values of HIX for A-WSOM showed a different change to that for M-WSOM, which was because of the similar decrease rate of C2 and C3 in the A-WSOM group.

4 DISCUSSION

4.1 Interaction of Fe, WSOM, and P Across pH Ranges

Compared with the adsorption of DOM and P onto Fe (hydr) oxides, coprecipitation of DOM-Fe-P is a much more important way to bury the element of C and P (Luo et al., 2021; Luo et al., 2022). Our experimental data show that pH has strong effects on the interaction of WSOM, Fe, and P, which may be explained by the species of Fe, WSOM, and P at diverse pHs and thus the effect of pH on the precipitation of iron and phosphate.

The coprecipitation mechanism of dissolved organic matter (DOM) with Fe(III) is regarded as the settling down of DOM which was caused *via* inclusion, occlusion, and adsorption (Eusterhues et al., 2011). Also, the structure of coprecipitates is proposed as a "layer-by-layer onion" model. The coprecipitates of phosphate with Fe(III) could be similar. Based on this mechanism, during the coprecipitation, phosphate could be adsorbed onto the surface of the iron (hydr)oxides and with the growth of coprecipitates, and some of the phosphates could be occluded in the inner layer of the coprecipitates. Thus, with the increase of pH, the surface charge of iron (hydr)oxides becomes more negative, which increases the repulsion between the phosphate anions and the surface sites and suppresses the removal of phosphate (Mallet et al., 2013).

For the ternary coprecipitation of WSOM-Fe-P, the effect of pH is similar to that in binary coprecipitation of Fe-P, which could be due to the similar mechanism of WSOM with Fe(III) to that of phosphate with Fe(III). OM is commonly rich in carboxyl and phenolic groups. The pKa values are 8.3–8.8 and 4.1 for the phenolic hydroxyl group (phenolic –OH) and carboxyl group (–COOH), respectively (Tipping et al., 2011). With the increase of pH from 6.5 to 8.5, more carboxyl groups (–COOH) are protonated, which facilitated the complexation reaction between carboxyl groups with Fe(III) to form stable complexes (Gu et al., 1994). In addition, the more ionized compound could facilitate the complexation of WSOM with Fe(III), as evidenced by the higher dissolved iron (**Figures 2A, C**) at pHs of 8.5 and 7.5 than those at pH of 6.5. This also suppressed the precipitation of Fe, as well as the coprecipitation of DOC and P with Fe(III).

4.2 Influence of WSOM Structure Differences on Coprecipitation With Fe and P in Two Typical Lake States

As discussed earlier, the presence of WSOM inhibits the reaction of Fe and P *via* 1) increasing the soluble complex Fe(III) and thus suppressing the precipitation of Fe; and 2) competing with phosphate to associate with Fe. More dissolved Fe in the A-WSOM group than in the M-WSOM group could be due to the more carboxyl groups in OM in algae-dominated sediments than in macrophyte-dominated sediments (Wen et al., 2022). In addition, the source and composition of WSOM showed an obvious effect on the sequestration of OC and P. Compared to A-WSOM, M-WSOM showed less inhibition on P sequestration (**Figure 3**) and stronger sequestration of OC (**Table 2**), which was related to the inherent properties and structure of WSOM. Our previous study showed that M-WSOM has higher aromaticity and molecular weight than A-WSOM (Du et al., 2022). It had been found that OM with a high humification degree or aromatic structure possessed a strong ability to coprecipitate with Fe(III) (Han et al., 2019; Luo et al., 2022).

The C/Fe ratios in coprecipitates (**Table 2**) showed that the coprecipitated OC in the M-WSOM group was about 1.4–1.6 times that in the A-WSOM group. Interestingly, the increased OC coprecipitation did not result in the less P in the coprecipitates when compared to the M-WSOM and A-WSOM groups as the P/Fe ratios in coprecipitates in the M-WSOM group were 1–3 times that in A-WSOM groups. Previous studies (Eusterhues et al., 2011; Han et al., 2019) suggested that the C/Fe ratio in coprecipitates strongly affected the reductive release of both

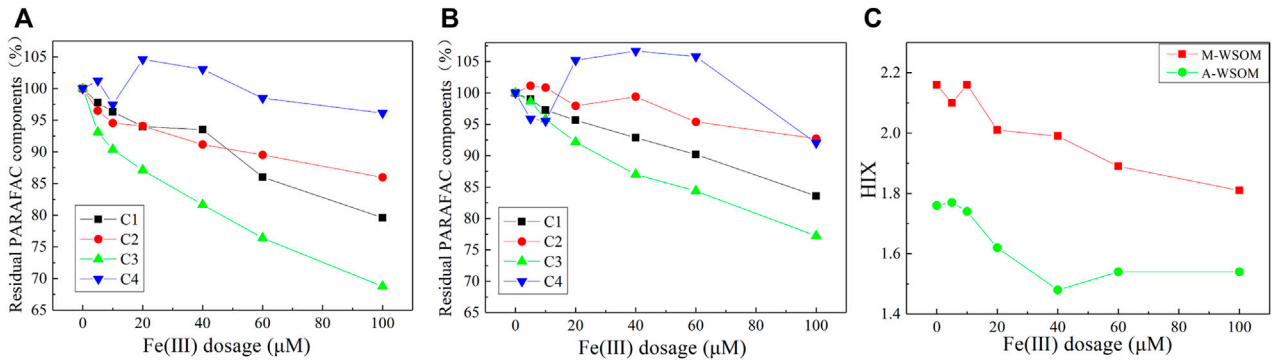

FIGURE 5 | Residual percentage of four PARAFAC components of M-WSOM **(A)** and A-WSOM **(B)** after coprecipitation under different Fe (III) dosages (pH = 6.5), and the effect of Fe (III) dosage on values of HIX of WSOM after coprecipitation with Fe and P (pH = 6.5) **(C)**.

Fe and OC, and coprecipitated OC at higher C/Fe ratios would be more resistant to release by reductive dissolution and may show higher stability. Iron-bound phosphorus in sediments of lakes is regarded as the mobile phosphorus since iron is readily reduced under anoxic conditions and thus releases the combined phosphorus (Sondergaard et al., 2001). Thus, although the coprecipitation of M-WSOM had a moderate inhibition effect (0.2–50%) on P immobilization, the accompanying WSOM in the coprecipitates could suppress the subsequent release of P. For A-WSOM, a relatively low C/Fe ratio might perform weak protection on the reduction of coprecipitates of A-WSOM with Fe-P. Moreover, the presence of A-WSOM inhibited the P immobilization significantly (74%, **Figure 3**). From these two aspects, there could be more dissolved phosphorus in the algae-dominated zone, which accelerates the growth of phytoplankton and thus the production of algae-derived OM. With the enhancement of the mobility of phosphorus by the algae-derived OM and vice versa, the production of algae-derived OM with more soluble phosphorus could perform positive feedback that serves as another pathway contributing to the internal P loading in lakes, besides the release of mobile Fe-P under the anoxic environment. The high internal P loading retards the restoration of eutrophic lakes despite rigorous control of external P loading (Sondergaard et al., 2003). Therefore, our findings provide a novel explanation for the difficulty to restore the eutrophic lake.

5 CONCLUSION

Our results showed that WSOM from the sediments in the two typical states of shallow lakes had a different composition and performed different competition to P during the coprecipitation process with Fe(III), which occurs frequently at the sediment–water interface. A-WSOM suppressed the precipitation of P and Fe. M-WSOM also showed a moderate inhibition of the precipitation of P. Moreover, the formed ternary coprecipitates with M-WSOM showed a higher ratio of C/Fe, and OM in the coprecipitates had more aromatic groups. Such coprecipitates could be more resistant to reducing and thus retarding P release. The stability of WSOM-Fe-P coprecipitates under anoxic conditions needs further investigation, which is crucial to understanding the potential release process of the iron-bound OC or phosphorus in two typical states of shallow lakes.

DATA AVAILABILITY STATEMENT

The raw data supporting the conclusion of this article will be made available by the authors, without undue reservation.

AUTHOR CONTRIBUTIONS

Conceptualization: YD. Data curation: JD and SW. Formal analysis: JL. Investigation: QZ and JD. Methodology: YD and YZ. Resources: YZ. Visualization: JD and QZ. Writing—original draft: JD and QZ. Writing—revision: YD and DH.

FUNDING

Funding for this work was provided through the National Natural Science Foundation of China (Nos 41971139, 41930760, and 41671099), the Natural Science Foundation of Jiangsu Province (BK20220015), and the Hong Kong Branch of Southern Marine Science and Engineering Guangdong Laboratory (Guangzhou) (SMSEGL20SC01), and the Center for Ocean Research in Hong Kong and Macau (CORE), a joint research center between the Qingdao National Laboratory for Marine Science and Technology and Hong Kong University of Science and Technology.

SUPPLEMENTARY MATERIAL

The Supplementary Material for this article can be found online at: https://www.frontiersin.org/articles/10.3389/fbioe.2021.715328/full#supplementary-material

REFERENCES

Chen, C., Dynes, J. J., Wang, J., and Sparks, D. L. (2014). Properties of Fe-Organic Matter Associations via Coprecipitation versus Adsorption. *Environ. Sci. Technol.* 48, 13751–13759. doi:10.1021/es503669u

Conley, D. J., Paerl, H. W., Howarth, R. W., Boesch, D. F., Seitzinger, S. P., Havens, K. E., et al. (2009). Controlling Eutrophication: Nitrogen and Phosphorus. *Science* 323, 1014–1015. doi:10.1126/science.1167755

Dean, W. E., and Gorham, E. (1998). Magnitude and Significance of Carbon Burial in Lakes, Reservoirs, and PeatLands. *Geol* 26, 5352–5538. doi:10.1130/0091-7613(1998)026<0535:Masocb>2.3.Co10.1130/0091-7613(1998)026<0535:masocb>2.3.co;2

Dittmar, T., Koch, B., Hertkorn, N., and Kattner, G. (2008). A Simple and Efficient Method for the Solid-phase Extraction of Dissolved Organic Matter (SPE-DOM) from Seawater. *Limnol. Oceanogr. Methods* 6, 230–235. doi:10.4319/lom.2008.6.230

Du, Y., Dai, J., Zhang, Q., Liu, J., Huang, X., An, S., et al. (2022). Spectroscopic and Molecular Characterization of Water Soluble Organic Matter from Sediments in the Macrophyte-Dominated and Algae-Dominated Zones of Taihu Lake (In Chinese). *J. Environ. Sci.* 43 (8), 4108–4117. doi:10.13227/j.hjkx.202112137

Eusterhues, K., Rennert, T., Knicker, H., Kögel-Knabner, I., Totsche, K. U., and Schwertmann, U. (2011). Fractionation of Organic Matter Due to Reaction with Ferrihydrite: Coprecipitation versus Adsorption. *Environ. Sci. Technol.* 45, 527–533. doi:10.1021/es1023898

Gu, B., Schmitt, J., Chen, Z., Liang, L., and McCarthy, J. F. (1994). Adsorption and Desorption of Natural Organic Matter on Iron Oxide: Mechanisms and Models. *Environ. Sci. Technol.* 28, 38–46. doi:10.1021/es00050a007

Han, L., Sun, K., Keiluweit, M., Yang, Y., Yang, Y., Jin, J., et al. (2019). Mobilization of Ferrihydrite-Associated Organic Carbon during Fe Reduction: Adsorption versus Coprecipitation. *Chem. Geol.* 503, 61–68. doi:10.1016/j.chemgeo.2018.10.028

Hashitani, H., and Okumura, M. (1987). A Simple Visual Method for the Determination of Phosphorus in Environmental Waters. *Z. Anal. Chem.* 328, 251–254. doi:10.1007/bf00481631

Kleber, M., Eusterhues, K., Keiluweit, M., Mikutta, C., Mikutta, R., and Nico, P. S. (2015). Mineral-Organic Associations: Formation, Properties, and Relevance in Soil Environments. *Adv. Agron.* 130, 1–140. doi:10.1016/bs.agron.2014.10.005

Lai, S., Wan, H., Tang, F., Yang, H., Huang, C., Zhang, Z., et al. (2020). Characteristics and Source Analysis of Organic Carbon Buried in Sediments of Fuxian Lake (In Chinese). *J. Environ. Sci.* 40, 1246–1256. doi:10.19674/j.cnki.issn1000-6923.2020.0087

Liu, S., He, Z., Tang, Z., Liu, L., Hou, J., Li, T., et al. (2020). Linking the Molecular Composition of Autochthonous Dissolved Organic Matter to Source Identification for Freshwater Lake Ecosystems by Combination of Optical Spectroscopy and FT-ICR-MS Analysis. *Sci. Total Environ.* 703, 134764. doi:10.1016/j.scitotenv.2019.134764

Luo, C., Wen, S., An, S., Lu, Y., and Du, Y. (2021). Phosphate Alters the Compositional Characteristics of Humic Acid Adsorbed onto Goethite. *J. Soils Sediments.* 21, 3352–3366. doi:10.1007/s11368-021-02973-4

Luo, C., Wen, S., Lu, Y., Dai, J., and Du, Y. (2022). Coprecipitation of Humic Acid and Phosphate with Fe(III) Enhances the Sequestration of Carbon and Phosphorus in Sediments. *Chem. Geol.* 588, 120645. doi:10.1016/j.chemgeo.2021.120645

Lützow, M. v., Kögel-Knabner, I., Ekschmitt, K., Matzner, E., Guggenberger, G., Marschner, B., et al. (2006). Stabilization of Organic Matter in Temperate Soils: Mechanisms and Their Relevance under Different Soil Conditions - a Review. *Eur. J. Soil Sci.* 57, 426–445. doi:10.1111/j.1365-2389.2006.00809.x

Mallet, M., Barthélémy, K., Ruby, C., Renard, A., and Naille, S. (2013). Investigation of Phosphate Adsorption onto Ferrihydrite by X-Ray Photoelectron Spectroscopy. *J. Colloid Interface Sci.* 407, 95–101. doi:10.1016/j.jcis.2013.06.049

McKnight, D. M., Boyer, E. W., Westerhoff, P. K., Doran, P. T., Kulbe, T., and Andersen, D. T. (2001). Spectrofluorometric Characterization of Dissolved Organic Matter for Indication of Precursor Organic Material and Aromaticity. *Limnol. Oceanogr.* 46, 38–48. doi:10.4319/lo.2001.46.1.0038

Mikutta, C., and Kretzschmar, R. (2008). Synthetic Coprecipitates of Exopolysaccharides and Ferrihydrite. Part II: Siderophore-Promoted Dissolution. *Geochimica Cosmochimica Acta* 72, 1128–1142. doi:10.1016/j.gca.2007.11.034

Scheffer, M., Carpenter, S., Foley, J. A., Folke, C., and Walker, B. (2001). Catastrophic Shifts in Ecosystems. *Nature* 413, 591–596. doi:10.1038/35098000

Scheffer, M., Hosper, S. H., Meijer, M.-L., Moss, B., and Jeppesen, E. (1993). Alternative Equilibria in Shallow Lakes. *Trends Ecol. Evol.* 8, 275–279. doi:10.1016/0169-5347(93)90254-M

Søndergaard, M., Jensen, J. P., and Jeppesen, E. (2003). Role of Sediment and Internal Loading of Phosphorus in Shallow Lakes. *Hydrobiologia* 506-509, 135–145. doi:10.1023/B:HYDR.0000008611.12704.dd

Sondergaard, M., Jensen, P. J., and Jeppesen, E. (2001). Retention and Internal Loading of Phosphorus in Shallow, Eutrophic Lakes. *Sci. World J.* 1, 427–442. doi:10.1100/tsw.2001.72

Sowers, T. D., Holden, K. L., Coward, E. K., and Sparks, D. L. (2019). Dissolved Organic Matter Sorption and Molecular Fractionation by Naturally Occurring Bacteriogenic Iron (Oxyhydr)oxides. *Environ. Sci. Technol.* 53, 4295–4304. doi:10.1021/acs.est.9b00540

Stedmon, C. A., and Bro, R. (2008). Characterizing Dissolved Organic Matter Fluorescence with Parallel Factor Analysis: A Tutorial. *Limnol. Oceanogr. Methods* 6, 572–579. doi:10.4319/lom.2008.6.57210.4319/lom.2008.6.572b

Stookey, L. L. (1970). Ferrozine---a New Spectrophotometric Reagent for Iron. *Anal. Chem.* 42, 779–781. doi:10.1021/ac60289a016

Tipping, E., Lofts, S., and Sonke, J. E. (2011). Humic Ion-Binding Model VII: A Revised Parameterisation of Cation-Binding by Humic Substances. *Environ. Chem.* 8, 225–235. doi:10.1071/en11016

Verpoorter, C., Kutser, T., Seekell, D. A., and Tranvik, L. J. (2014). A Global Inventory of Lakes Based on High-Resolution Satellite Imagery. *Geophys. Res. Lett.* 41, 6396–6402. doi:10.1002/2014GL060641

Wang, W., Dou, W., He, C., and Shi, Q. (2020). Characterization of Surface Water Dissolved Organic Matter by Stepwise Elution Solid Phase Extraction Followed by Fourier Transform Ion Cyclotron Resonance Mass Spectrometry(in Chinese). *Chin. J. Analysis Laboratory* 39, 521–526.

Wen, S., Lu, Y., Luo, C., An, S., Dai, J., Liu, Z., et al. (2022). Adsorption of Humic Acids to Lake Sediments: Compositional Fractionation, Inhibitory Effect of Phosphate, and Implications for Lake Eutrophication. *J. Hazard. Mater.* 433, 128791. doi:10.1016/j.jhazmat.2022.128791

Yamashita, Y., and Jaffé, R. (2008). Characterizing the Interactions between Trace Metals and Dissolved Organic Matter Using Excitation–Emission Matrix and Parallel Factor Analysis. *Environ. Sci. Technol.* 42, 7374–7379. doi:10.1021/es801357h

Zhou, L., Zhou, Y., Yao, X., Cai, J., Liu, X., Tang, X., et al. (2020). Decreasing Diversity of Rare Bacterial Subcommunities Relates to Dissolved Organic Matter along Permafrost Thawing Gradients. *Environ. Int.* 134, 105330. doi:10.1016/j.envint.2019.105330

Zsolnay, A., Baigar, E., Jimenez, M., Steinweg, B., and Saccomandi, F. (1999). Differentiating with Fluorescence Spectroscopy the Sources of Dissolved Organic Matter in Soils Subjected to Drying. *Chemosphere* 38, 45–50. doi:10.1016/s0045-6535(98)00166-0

Conflict of Interest: The authors declare that the research was conducted in the absence of any commercial or financial relationships that could be construed as a potential conflict of interest.